Received: October 23, 2024. Revised: December 1, 2024.

International Journal of
Intelligent Engineering & Systems

http://www.inass.org/

A Hybrid Deep Learning and Machine Learning Model for Multi-Class Lung Disease Detection in Medical Imaging

Mustafa Abdul Salam[1]* **Amr Abdellatif[2]** **Marwa Abdallah[2]** **Nabil Abdul Salam[3]**

[1] *Department of Computer Engineering and Information, College of Engineering, Wadi Ad Dwaser, Prince Sattam Bin Abdulaziz University, Al-Kharj 16273, Saudi Arabia*
[2] *Computer Science Department, Faculty of Computers and Information, Zagazig University, Zagazig 13511, Egypt*
[3] *Computer Science Department, Higher Technological Institute, Cairo 11331, Egypt*
* Corresponding author's Email: m.aboelnour@psau.edu.sa

Abstract: Lung diseases encompass a broad range of conditions that affect the respiratory system, driven by factors such as genetic predisposition, environmental pollution, infections, and smoking. Early detection is essential for effective treatment and improved patient outcomes. This paper introduces an innovative framework that combines deep learning (DL) and machine learning (ML) models to autonomously detect and classify lung diseases using medical images from volumetric datasets. The proposed model aims to classify lung cancer into subtypes, including adenocarcinoma, squamous cell carcinoma, and large cell carcinoma, while also distinguishing between pneumonia and COVID-19. Convolutional Neural Networks (CNNs) are employed for feature extraction, demonstrating strong performance when applied to biomedical image datasets, such as the COVID-19 Radiography Database from Kaggle. A 2D CNN model is used in this study to efficiently extract features while reducing computational overhead. These CNN-extracted features are then classified using various machine learning algorithms, including Random Forest, Adaboost, and Voting classifiers. The hybrid model showed robust performance across diverse testing scenarios, highlighting its potential for practical applications and establishing it as a valuable tool for the automated detection and classification of lung diseases.The datasets employed in this study are sourced exclusively from open-access datasets available on the Kaggle website contains 32,975 images of CT-scan and CXR types with dimensions of 224 × 224. Notably, the hybrid CNN-ML classifier achieved high accuracy in identifying pneumonia, with a recall of 0.94, precision of 0.98, and F1-score of 0.96. For COVID-19, the CNN classifier yielded a recall, precision, and F1-score of 0.94 across all metrics. The hybrid approach can accurately detect and categorize lung diseases, particularly pneumonia, and suggest its potential for broader medical use. By integrating a Random Forest classifier with a Convolutional Neural Network, the proposed model demonstrated a significant improvement in accuracy, reaching 89% compared to the baseline CNN's 85.4%.

Keywords: Deep Learning (DL), Machine Learning (ML), Convolutional Neural Networks (CNNs), Lung diseases, Random Forest (RM), Adaboost, Voting.

1. Introduction

The lungs play a critical role in the human body because they allow for the expansion and contraction necessary for the absorption of oxygen and the outflow of carbon dioxide. Respiratory diseases encompass a range of conditions impacting the organs and tissues involved in breathing. These conditions span airway ailments, lung tissue disorders, and lung circulation irregularities. Certain respiratory issues, such as influenza, result in minor discomfort and disruptions, whereas others like pneumonia, COVID-19, tuberculosis, lung opacity and lung cancer pose life-threatening risks and give rise to significant acute respiratory challenges [1-3].

COVID-19 and pneumonia have posed a serious global health risk, leading to a vast number of infections and deaths. According to the World Health Organization (WHO), there have been over 770 million confirmed cases and more than 6.9 million fatalities worldwide due to these diseases. [4]. In the year 2019, pneumonia was linked to 740,180 cases of child mortality. Notably, 14% of all deaths from pneumonia occur in children under the age of 5 years [5]. Lung cancer poses a noteworthy issue in public health, resulting in a substantial global death toll. According to the cancer incidence and mortality projections from GLOBOCAN 2020, The International Agency for Research on Cancer (IARC) has reported that lung cancer continues to be the leading cause of cancer deaths globally, with approximately 1.8 million people losing their lives to the disease in 2020. This represents 18% of all cancer-related fatalities worldwide.[6].

Early detection considerably increases the likelihood of a successful recovery and raises the percentages of long-term survival [7]. Skin testing, blood tests, sputum sample evaluations, chest X-ray investigations, and CT scans were once used to diagnose lung conditions. Modern times have seen potential improvements in the application of DL models to the field of medical image analysis, especially lung problems. To evaluate the scanned photos and identify the illnesses, qualified professionals must be present. In rural Community Health Centers (CHCs), there is a shortage of 76.1 percent of physicians, according to data from the Union Health Ministry [8]. On the other hand, A hurdle associated with chest X-ray (CXR) images lies in their potential complexity during interpretation, owing to the presence of diverse degrees of interference like noise, artifacts, and other irregularities. Moreover, the subtle distinctions between CXR images depicting normal and abnormal conditions can pose difficulties in differentiation, resulting in subjective and potentially unreliable diagnoses. Deep learning (DL) techniques are used to get around this, opening the door for a fresh approach.

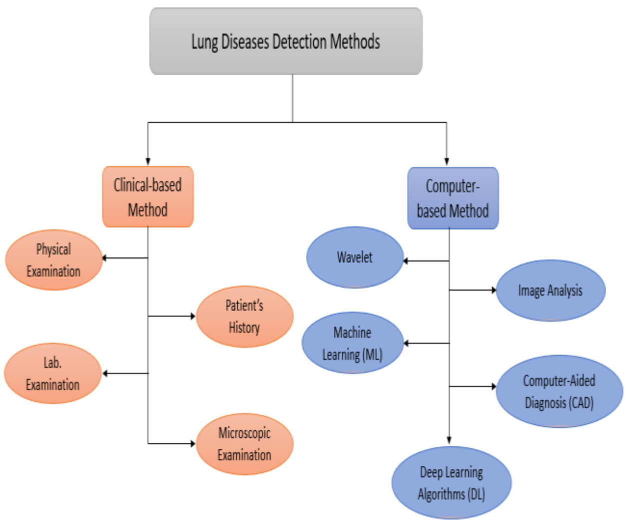

Figure. 1 The Classification of Lung Diseases Diagnosis Methods

The techniques utilized for diagnosing respiratory system diseases can be broadly categorized into two main groups: computer-based and clinical techniques, as illustrated in Fig. 1. Clinical evaluation approaches encompass four distinct methods: conventional physical examination, review of patient medical history, laboratory testing, and microscopic analysis. In contrast, computer-assisted diagnostic techniques can be further segmented into five prevalent strategies, which include wavelet analysis, image interpretation, utilization of ML methods, and the application of DL algorithms.

Researchers from all over the world have already carried out numerous studies that have produced encouraging findings in the detection of diseases. These studies can support current approaches or pave the way for new ones that weren't previously possible. These developments can help in the fast and precise diagnosis and classification of diseases, particularly lung disorders, and can offer immediate support to achieve outstanding outcomes in eliminating fatal infectious diseases [9-11]. DL constitutes a subset of ML focused on algorithms that draw inspiration from the operation and organization of the human brain. Rapidly advancing to the forefront, deep learning is elevating itself as a state-of-the-art technique, resulting in enhanced performance across various medical applications. DL techniques such as the CNNs have gave attention for their ability to enhance accuracy and automate feature extraction in lung diseases detection. However, these methods face significant challenges in terms of extended processing times and substantial space prerequisites when it comes to automatic feature learning and estimation from input images. The present methods assign both feature extraction and classification tasks to CNNs, contributing to the increased time and space requirements [12, 13].

For this reason, this paper proposed a hybrid DL with ML model for lung diseases diagnosis such as pneumonia, COVID-19, lung opacity and lung carcinoma. This proposed hybrid model is also utilized to classify the lung carcinoma into three types which are adenocarcinoma, squamous cell carcinoma, and large cell carcinoma. The proposed model created 2D CNN layers that help to reduce the processing time needed for the automatic extraction of CNN features. A variety of classifiers were used to the CNN outputs for the identification and classification of lung illnesses to overcome the problems of gradient vanishing and elevated computational obligations. In this study, the following contributions are introduced:

- The suggested hybrid DL and ML enhanced detection of lung diseases, especially detection and classification of lung diseases.
- A reliable 2D CNN is outlined for effective feature extraction of different lung diseases.
- ML classifiers have been employed for diseases classification such as Linear Regression and Random Forest (RM).

In summary, the paper's approach aims to significantly improve the diagnosing and classifying lung diseases, providing a good tool for medical professionals, and potentially overcoming challenges associated with traditional diagnostic methods.

The proposed model leverages a 2D-CNN as a robust feature extractor, followed by a multi-classifier ensemble comprising Random Forest, Adaboost, and Voting classifiers for accurate multi-class classification.

The structure of the paper is outlined as follows: In Section 2, there is an exposition of related studies concerning classification or the detection and categorization of lung diseases. The methodology is expounded upon in Section 3. Findings and the ensuing discourse are offered in Section 4, and the paper concludes with Section 5.

2. Related works

Different applications use a variety of DL methods since the algorithms used depend on the type of data being used. Following the successful introduction of GPUs and DL algorithms, there was a significant surge in the efficacy of CAD systems for lung disease detection and decision support mechanisms [14-38]. Numerous research studies have put forth various deep learning models aimed at detecting lung cancer and other lung diseases. This section will discuss many searches that help to detect lung diseases at early stages.

The researchers in [14] suggested utilizing a combination of two CNNs, specifically RetinaNet and Mask R-CNN, to identify and pinpoint instances of pneumonia. To assess the effectiveness of their approach, they employed a dataset with 26,684 images. Impressively, their method ranked in the top 3% of submitted solutions. Achieving a recall rate of 0.793, the authors successfully created a dependable automated diagnosis solution for pneumonia, which they put to the test on the most extensive clinical database available to the public up to that point.

In [15], The authors compared several CNNs architectures for their ability to automatically classify pneumonia images. The comparison was based on the performance of these models in binary classification tasks. The outcomes of the experimentation led the authors to the conclusion that the ResNet50 model exhibited good performance.

The research [16] introduced CNN model, designed for the purpose of diagnosing typical pneumonia (both bacterial and viral) as well as COVID-19 the proposed model achieved an impressive accuracy of 97.60%. Moreover, the model exhibited sensitivities of 100%, 96.30%, and 96.58% in detecting cases.

The study by Rahman et al. [17] used data augmentation, and DL-based classification techniques to accurately detect tuberculosis in CXR images. They employed nine different CNNs for transfer learning, using the NIAID TB dataset and the RSNA dataset for training and evaluation. They used segmentation which improved the accuracy.

To address the challenge of sparse data, Lin et al. [18] introduced the Generative Adversarial Network (GAN) as a solution to generate lung cancer computed tomography (CT) images. GAN is harnessed to autonomously produce novel data by training both the generator and discriminator networks concurrently. The outcome demonstrated an exceptional accuracy of 99.86%.

The study by Ashhar et al. [19] compared the performance of five different CNNs on CT images. The goal was to classify lung tumors into two categories. The results showed that GoogleNet outperformed the other architectures.

The authors in [20, 21] introduced DL models to detect COVID-19 at early stages. The authors have devised a dual-sampling approach aimed at alleviating imbalanced learning challenges. This approach underwent evaluation on the most extensive multi-center CT dataset for COVID-19, encompassing data from eight different hospitals. The outcomes revealed that the proposed algorithm achieved a detection accuracy of 87.5% for identifying COVID-19 images.

In [22], The study employed DL techniques to produce accurate models for detecting COVID-19 in CXR images. These models combined CNNs, transfer learning models, and ML classifiers to enhance their performance. This model gave 97.8% accuracy for multiclass model.

In [23], The authors of the study proposed a medical recommender system that uses an IoT device to treat chronic diseases. They employed the KNN method to the proposed method has high accuracy in predicting chronic diseases and outperforms previous methods.

In [24], The authors of the study proposed a novel

Received: October 23, 2024. Revised: December 1, 2024.

Table 1. The Summary of Literature Review

Authors/ Ref.	***Year***	***Disease Name***	***Medical Image Type***	***Objective***	***Dataset***	***Used Algorithm***	***Evaluation Parameters***
Sirazitdinov et al. [14]	2019	Pneumonia	CXR Images	Detection & Localization	RSNA Pneumonia Detection Challenge dataset	RetinaNet and Mask R-CNN	Recall 79.3%
K. El Asnaoui et al. [15]	2021	Pneumonia	CXR & CT Images	Detection & Classification	COVID-19 image data collection, Mendeley Chest x-ray images.	CNN	Accuracy 96% Sensitivity 94.92%
H. C. Reis et al. [16]	2022	Pneumonia & COVID-19	CXR & CT Images	Detection & Classification	A COVID multiclass dataset of CT scans COVID-19 and common pneumonia chest CT dataset	CNN	Sensitivity 96.58%
T. Rahman et al. [17]	2020	TB	CXR Images	Lung Segmentation & TB classification	NLM dataset RSNA dataset	CNN	96.47% Accuracy
C. H. Lin et al. [18]	2021	Lung Cancer	CT Images	Classification	SPIE-AAPM Lung CT Challenge Dataset	CNN pre-trained on AlexNet	Accuracy 99.86%
S. M. Ashhar et al. [19]	2021	Lung Cancer	CT Images	Detection & Classification of lung lesions	Lung Image Database Consortium image collection (LIDC-IDRI)	CNN pre-trained on (GoogleNet SqueezeNet, ShuffleNet,)	Accuracy 94.53% Sensitivity 65.67%
X. Ouyang et al. [20]	2020	COVID-19	CT Images	Detection & Classification of COVID-19 and CAP infection	COVID-19 CT Images were provided by the Tongji Hospital of Huazhong University of Science and Technology, Shanghai Public Health Clinical	CNN	Accuracy 87.5% Sensitivity 86.9% Specificity 90.1% F1-score of 82.0%
M. Ahsan et al. [21]	2020	COVID-19	CXR & CT images	Detection	Open-source GitHub COVID-19 repository shared by Dr. Joseph Cohen	MLP-CNN (Adam, Sgd, and Rmsprop)	Higher accuracy of 96.3% using Adam
T. S. Qaid et al. [22]	2021	COVID-19 and pneumonia	CXR Images	Detection	COVID-19 Radiography Database from Kaggle and a local data set from Asir Hospital, Abha, Saudi Arabia.	Hybrid CNN + ML	Higher accuracy of 99.82%
Y. A. Nanehkaran et al. [23]	2022	Chronic disease	CT images	Detection	PhysioNet	KNN	Accuracy 96.5%
Xinrong Lu et al. [24]	2021	Lung Cancer	CT images	Detection	RIDER dataset	CNN ResNet-18	Accuracy 93.4%

Received: October 23, 2024. Revised: December 1, 2024.

							sensitivity 98.4%
G.V. Eswara Rao et al. [25]	2024	COVID-19	CXR Images	Detection	COVID-19 Radiography Dataset	CNN , MMS	Accuracy 98.9 %
P.Ramadevi et al. [26]	2024	COVID-19	CXR Images	Detection & Classification	Kaggle repository	CNN,SVM	Accuracy 98.7 %

methodology for early cancer detection using image processing, DL, and a metaheuristic algorithm. They designed a new CNN and employed the marine predator's algorithm to optimize its structure and enhance its accuracy. The proposed method outperformed the compared techniques, achieving an accuracy of 93.4%.

In [25], The authors proposes a hybrid respiratory lung disease detection framework based on classical CNN and Quantum classifiers. It combines a classical deep feature extraction model with quantum classifiers. The experimental results revealed that the proposed model had the highest training and testing accuracy of 98.9% and 98.1%

In [26], The authors investigates the optimization of CNN hyperparameters using Bayesian methods and their integration with SVM kernels for CXR image classification. We compared six pre-trained deep learning models (AlexNet, ResNet50, ResNet101, VGG16, VGG19, InceptionV3) with our optimized CNN-SVM model The results demonstrate that the proposed approach, particularly the ResNet101 model with the SVM kernel, achieves the highest accuracy of 98.7%.

We can enhance the existing methods as follows:

- Divide the lung into anatomically relevant segments to facilitate accurate CNN feature extraction.
- Conduct extensive experimentation with various CNN and RNN architectures, including convolutional layers, recurrent layers, and attention mechanisms.
- Optimize hyperparameters such as learning rate, batch size, and number of epochs to achieve optimal performance.
- Adapt the existing method to reduce computational complexity and latency, making it suitable for real-time clinical applications.

Table 1 introduces some of lung diseases detection DL models summary with their achieved results.

3. Proposed methodology

The proposed framework integrates 2D-CNN for feature extraction with several ML classifiers, including Random Forest (RF), Adaboost, and Voting classifiers. The dataset used in this study is the COVID-19 Radiography Database from Kaggle, which includes chest X-ray images categorized into seven classes: pneumonia, COVID-19, lung opacity, adenocarcinoma, squamous cell carcinoma, large cell carcinoma, and normal.

The steps of the proposed multi-classification hybrid model for lung diseases detection. The flowchart representation of the proposed method's workflow can be observed in Fig. 2. The presented architecture in Fig. 2 describes the steps of the proposed system for lung disease detection, involving primary stages such as medical image pre-processing, CNN feature extraction, and classification. To enhance quality, the initial step involves preprocessing each input medical image (CXR or CT images) using optimal filtering and contrast adjustment methods. We need our proposed model to classify the input medical images into normal, pneumonia, COVID-19, lung opacity or lung cancer. On the other hand, the proposed model helps to classify lung carcinoma into three types which are adenocarcinoma, squamous cell carcinoma, and large cell carcinoma. We used two basic blocks for building our model, which are DL and ML blocks. Given that machine learning techniques necessitate extracted features for successful classification tasks, the approach was taken to acquire these features from a robust technique such as deep learning. In this model, features were extracted through a CNN and subsequently supplied to one of the machine learning techniques. This hybrid model combined two components, CNN and machine learning (CNN-ML), with one serving as a feature extraction unit and the other dedicated to the classification process. The multi-classification process includes more than one classifier which are Random Forest (RM), Adaboost, and Voting ensemble classifier.

Received: October 23, 2024. Revised: December 1, 2024.

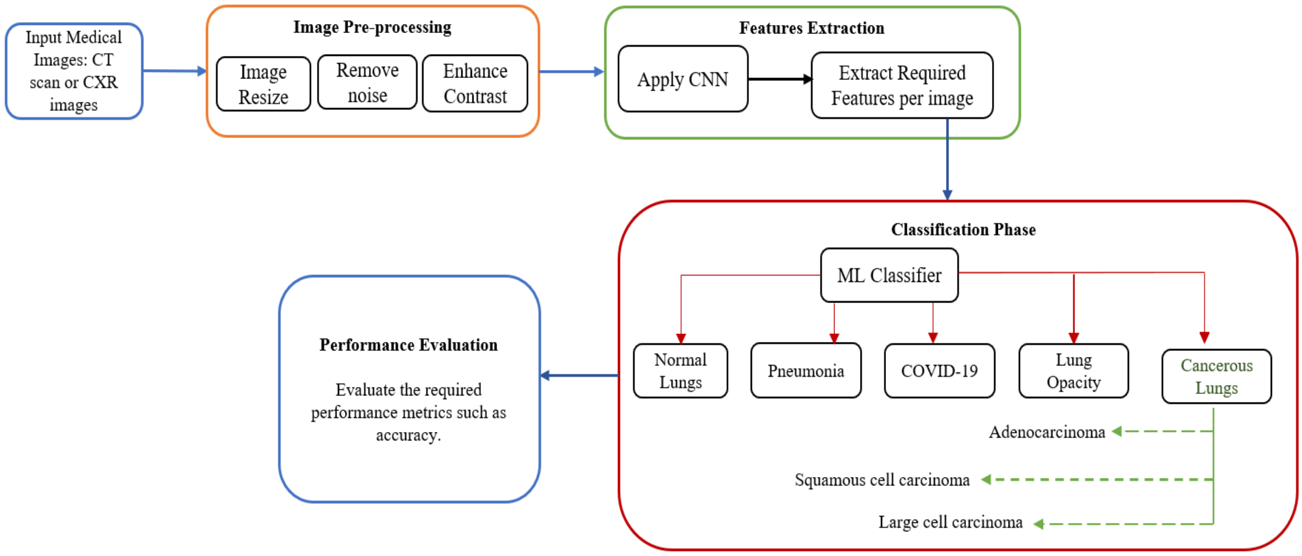

Figure. 2 The Flowchart of the proposed Hybrid DL and ML for Lung Diseases Detection

3.1 The collected medical dataset

The datasets employed in this study are sourced exclusively from open-access datasets available on the Kaggle website [27]. This paper collected different available datasets of pneumonia, COVID-19, normal and lung carcinoma which included three different datasets of adenocarcinoma, squamous cell carcinoma, and large cell carcinoma. This collected dataset contains 32,975 images of CT-scan and CXR types. In the initial layer, we supplied the pre-processed chest X-ray image with dimensions of 224 × 224 as input to the network. The pneumonia dataset contains 5,610 CXR images. The COVID-19 dataset that is used in this paper was composed from COVID-19 Radiography Database (Kaggle) [28, 29]. This data contains 8,722 medical images of CT scan and CXR images. The lung opacity dataset contains 6,012 CXR images The collected normal dataset contains around 11,923 CT scan and CXR images. For lung cancer dataset, there were 310 CT-scans of adenocarcinoma, 242 CT-scans of squamous cell carcinoma, and 156 CT-scans of large cell carcinoma.

Table 2 provides comprehensive information regarding the datasets that were utilized.

3.2 Image pre-processing

In medical imaging, achieving consistent brightness distribution across images is paramount for accurate analysis and diagnosis. However, inherent randomness in brightness levels can introduce unwanted

fluctuations, thereby compromising image fidelity and introducing visual disturbances.

The efficacy of a neural network in classifying medical images heavily relies on the quality of the dataset used for training. By employing meticulous image pre-processing techniques, we can mitigate noise and disturbances, enabling the neural network to focus on relevant features crucial for accurate diagnosis.

Our proposed model for the detection of lung diseases embarks on the journey of image preprocessing as a foundational step. This involves a

Table 2. The Collected Dataset

Properties	***Pneumonia***	***COVID-19***	***Lung Opacity***	***Lung Cancer***			***Normal***
				Adenocarcinoma	***squamous cell***	***Large Cell***	
Type	*CXR images*	*CT-scans & CXR images*	*CXR images*	*CT-scans*	*CT-scans*	*CT-scans*	*CT-scans & CXR images*
Number of images	*5,610*	*8,722*	*6,012*	*310*	*242*	*156*	*11,923*
Size	*224 × 224*	*224 × 224*	*224 × 224*	*224 × 224*	*224 × 224*	*224× 224*	*224 × 224*

sequence of operations such as normalization, noise removal, and enhancement, meticulously applied to each medical image within the dataset. Prioritizing image quality, we ensure that only pristine, denoised images progress to the subsequent stages of analysis, thereby optimizing the neural network's capacity to extract meaningful features.

To further fortify image fidelity, we harness computer-based techniques to artificially augment image quality. Data augmentation emerges as a pivotal strategy to enhance model performance by introducing variations in the dataset, thereby mitigating over fitting and fostering improved generalization during training. By enhancing image quality through targeted

Interventions, we not only bolster the model's predictive capabilities but also extend the applicability of medical imaging across diverse scenarios.

In essence, the pursuit of comprehensive and accurate image generalization underscores our commitment to advancing the frontier of medical imaging, empowering clinicians with robust tools for precise diagnosis and treatment planning.

3.3 The proposed DL features extractor

The method used for feature extraction significantly impacts the performance of the classification process. It represents a crucial step in comprehending the features within lung cancer histology images. The fundamental concept behind deep learning (DL) involves building a nonlinear network architecture. It begins by initializing weights using unsupervised methods and subsequently fine-tunes them through supervised training. The issue of gradient vanishing is effectively mitigated with the use of the ReLU activation function. DL gradually elevates the initial low-level features to high-level features through multi-layer processing, which proves advantageous for tackling intricate tasks, including image [30], speech [31], and language [32] processing. Our chosen approach involves employing DL, where the attributes of an image are automatically detected based on individual pixels. This approach aligns with the concept of CNNs, where convolution operations conduct discrete spatial processing calculations in an efficient manner [33]. CNNs are adept at automatically extracting relevant features from medical images. In the case of lung diseases, they can detect intricate patterns, textures, and structures within X-rays, CT scans, or histopathology images.

The CNN is used to extract important features from medical images related to lung diseases. The architecture of the CNN consists of layers used for image recognition and classification. Before reaching the fully connected layer, both training and testing data pass through filters like max-pooling and kernel filters. The ReLU activation function is used in all hidden layers. Fig. 3 shows the detailed structure of the CNN, with the layers and parameters set as follows:

- Input Layer: This initial layer serves as the entry point for the data, receiving and transmitting it to the first convolutional layer. In this scenario, the input consists of a 224 × 224-pixel CT-scan or CXR images.
  Convolution Layer: To capture the spatial structure of the images, this layer convolves the input image using trainable filters. This layer utilizes a variety of kernels to perform convolution operations on the feature vectors, resulting in the extraction of high-level semiotic information. The model includes three convolutional layers (CL) with kernels of sizes 64, 128, and 256. The series of CL layers employ a (3 × 3) kernel size, a stride of 4, and consistent padding. The ReLU activation function is applied to enhance performance in nonlinear operations. Moreover, the Adam optimizer was included in this study.
- Pooling Layer (PL): A max-pooling process is used to down-sample the output images from the convolution layers. After each CL layer, a max pooling layer with a (2 × 2) kernel size is applied. All pooling layers utilize the widely adopted max pooling operation.
- Fully Connected (FC) Layer: This layer has transformed the output from the convolutional layer into a one-dimensional vector. Following a sequence of convolution, activation, and pooling operations, the FC layer concatenates the features extracted from the last CL and the last max-PL into one vector.

Finally, the output vector of FC layers within the CNN will be input to a ML classifier, which will undergo training using this automatically extracted feature vector. Table 3 provides a summary of the parameters employed in this study for all used data sets.

Now the mathematical model of the CNN as a feature extractor will be illustrated. Let O` denotes the out of convolutional layers, and it can be expressed as:

$$\mathrm{O}^{\mathrm{CL}} = \mathrm{f}\left(\mathrm{b}^{\mathrm{CL}} + \sum_{\mathrm{j}}^{\mathrm{J}} \sum_{\mathrm{i}}^{\mathrm{I}} \mathrm{w}_{\mathrm{i,j}}^{\mathrm{CL}} \mathrm{O}_{\mathrm{i,j}}^{\mathrm{CL}-1}\right) \quad (1)$$

Received: October 23, 2024. Revised: December 1, 2024.

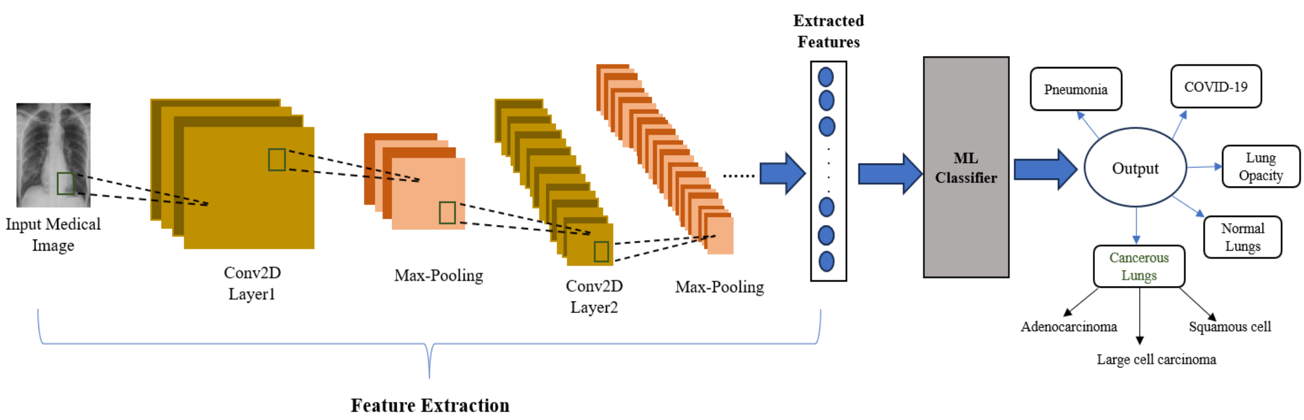

Figure. 3 The CNN Structure

Table 3. Parameters setting for proposed model

Parameter	***Applied value***
Input image size	224 × 224
Activation Function	ReLU
Kernel Size	*3x3*
Max-Pooling filtering Size	*2x2*
Stride Number	*4*
Padding	*Same*
Optimizer	*Adam*
Learning rate	*0.001*
Dropout rate	*0.5*
Number of convolution layer	*4*
Early stopping	*Enabled*

$$f(O^{CL}) = \mathrm{ReLU}\,(O^{CL}) = \begin{cases} O^{CL}, & O^{CL} > 0 \\ 0\,, & O^{CL} \leq 0 \end{cases} \quad (2)$$

Where b^{CL} represents the bias associated with the convolutional layer. Here, J and I represent the dimensions of the filters, with J being the height and I being the width of the filters. $w_{i,j}^{CL}$ stands for the convolutional layer's weight. $O_{i,j}^{CL-1}$ represents the output from the preceding convolutional layer. The activation function used is denoted as $f(O^{CL})$, and in this case, the ReLU activation function has been chosen. On the other hand, the max-pooling method employed in this paper is defined as follows:

$$y_j = \max_{NxN}(y^{NxN}x(n,n)) \quad (3)$$

Here, the function $x(n,n)$ represents the window function utilized to compute the maximum value of y_j within the surrounding neighborhood. Finally, the output extracted features vectors can be obtained by:

$$v^{FC} = f(w^{FC}O^{FC}) + b^{FC} \quad (4)$$

Where, w^{FC} represents the weights of the fully connected layer, while O^{FC} signifies the output derived from the preceding max-pooling layer. b^{FC} stands for the bias associated with the fully connected layer and the activation function employed here is denoted as $f(..)$, which is the ReLU activation function.

3.4 Classification using ML classifiers

The feature classification component in our suggested system differentiates instances between pneumonia, COVID-19, lung opacity, and normal. The proposed model can also be used to classify lung cancer into adenocarcinoma, squamous cell carcinoma, and large cell carcinoma. To classify the medical input images, we employed various classifiers including Random Forest (RF), Adaboost, and Voting ensemble between RF and Adaboost. Finally, CNN has been applied as a classifier also to compare between the results of ML classifiers and CNN as a classifier.

Random Forest (RF) [34], introduced by Breiman as an ensemble technique for classification tasks, enhances system accuracy by amalgamating multiple models to address the given problem. In typical scenarios, employing multiple decision models often yields less accurate predictions compared to those obtained with a single model. However, RF stands out as a premier machine learning algorithm for classification challenges across diverse research fields [11, 33, 35]. Its ability to draw training data from randomly selected subsets and construct trees in a similarly stochastic manner makes it particularly powerful [36]. Recent research demonstrates that random forest classifiers consistently deliver promising outcomes in various healthcare systems [35, 37].

The AdaBoost [38], is a ML technique employed as an Ensemble Method. It functions as a meta-algorithm classifier that trains multiple weak classifiers and assigns the same initial weight to each sample. It uses the multiclass TotalBoost algorithm. The concept behind the AdaBoost algorithm involves aggregating the outputs of several 'weak' classifiers (sub-classifiers) with weighted contributions to create a robust classification. Its flexibility stems from the fact that instances misclassified by the preceding sub-classifier are given increased importance through higher weights, and these weighted instances are subsequently utilized in retraining the next sub-classifier.

The voting ensemble leverages both mean aggregation and weighted majority voting, selecting the highest probability value for the target label. This approach effectively mitigates the limitations of individual classifiers by combining their outputs. Ensemble methods serve the purpose of minimizing bias and variance in individual classifiers, while also affording the opportunity to explore diverse parameter settings from the base classifiers. Additionally, it introduces structural diversity and multi-objective optimization, representing a remarkable advancement in this methodology [39]. This paper applied voting ensemble between RF and Adaboost.

Finally, this paper has applied CNN as a classifier to lung diseases. CNNs can be trained to classify lung diseases into multiple categories, which is particularly valuable for distinguishing between different types and stages of lung conditions [40]. CNNs are primarily designed to work with two-dimensional data, such as images. The input to a CNN is an image or a grid of pixels, represented as a matrix. CNNs consist of multiple layers, including CLs, PLs, and FC layers. These layers are stacked in a sequential manner. To train CNN for classification, a labeled dataset is used. The network learns to recognize patterns and features within the images that are associated with specific classes or categories. After training, CNN can be used for inference. When presented with a new, unlabeled image, the network processes the image through its layers and produces a probability distribution over the possible classes. The class with the highest probability is considered the prediction or classification result.

4. Experimental results and discussion

The hybrid proposed model has been implemented using the MATLAB Language. This section introduces and discusses the results of the proposed multi-classification hybrid (DL) and (ML) model that aims to autonomously differentiate between pneumonia, COVID-19, Lung opacity normal, and classify the lung cancer cases into adenocarcinoma, squamous cell carcinoma, and large cell carcinoma using chest medical images from volumetric datasets.

4.1 Evaluation metrics

Numerous evaluation metrics, including accuracy, recall, precision, F1-score, AUC (Area Under Curve), and ROC graphs, are employed to quantitatively assess the effectiveness of the proposed method. These metrics rely on four essential calculations: accurately detected unhealthy cases.

Accuracy: One of the most utilized and fundamental performance metrics is accuracy, representing the likelihood that a randomly chosen example (either negative or positive) will yield a correct result. In the context of this metric, the diagnostic test indicates the probability of obtaining a correct outcome, signifying the probability of an accurate diagnosis.

$$\text{Accuracy} = \frac{\text{TP} + \text{TN}}{\text{TN} + \text{FP} + \text{FN} + \text{TP}} \tag{5}$$

Recall, also referred to as sensitivity, true positive rate, or hit rate, gauges a model's ability to identify all positive cases (TP). It's important to observe that the equation mentioned above implies that a high recall typically corresponds to a low false-negative (FN) rate. It can be determined as in Eq. (6).

$$\text{Recall} = \frac{\text{TP}}{\text{TP+FN}} \qquad (6)$$

Precision: is the proportion of True Positives relative to all Positive cases. In our specific context, it signifies the ability to accurately identify patients with a particular lung disease among all patients who genuinely have it. It can be determined as in Eq. (7).

$$\text{Precision} = \frac{\text{TP}}{\text{TP+FP}} \qquad (7)$$

F1-Score: While not as intuitive as accuracy, this metric serves as a valuable indicator of the classifier's precision and resilience. The F1 score, a crucial measure of test performance that takes both recall and precision into account, is commonly calculated as a weighted average of these two metrics.

$$\text{f}_1 - \text{score} = \frac{2 \times \text{TP}}{(2 \times \text{TP}) + \text{FP} + \text{FN}} \qquad (8)$$

4.2 Results analysis

This research assesses the efficiency of the proposed multi-classification hybrid model for the detection of lung diseases using the collected dataset described before. The proposed scheme divided the image into six categories which are pneumonia, COVID-19, lung opacity, normal, and classify the

Table 4. Accuracy Results Comparison

MModel	CNN	CNN-Adaboost	CNN-voting	CNN-RF
AAccuracy (%)	85.4	87.3	88	**89**

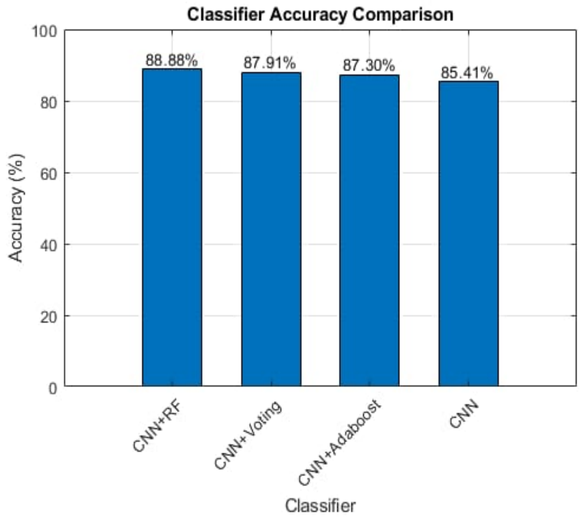

Figure. 4 The Graphical representation of the Accuracies of all classifiers

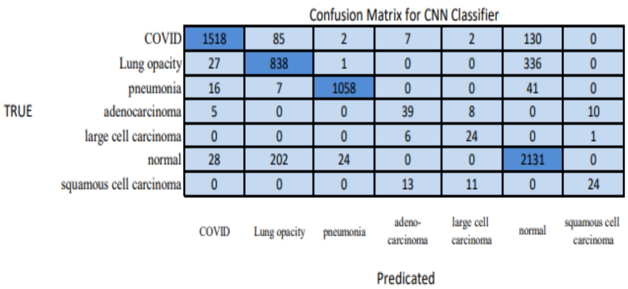

(a)

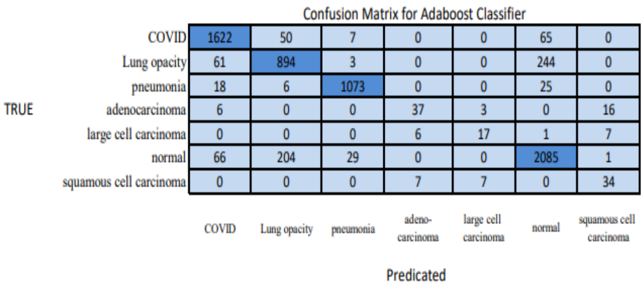

(b)

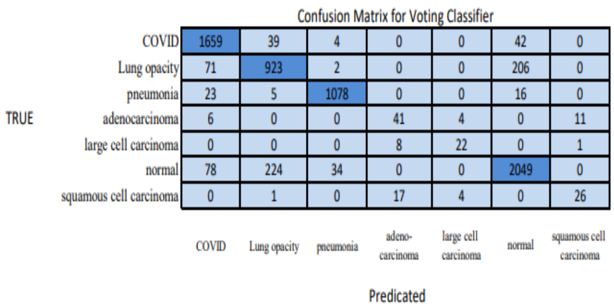

(c)

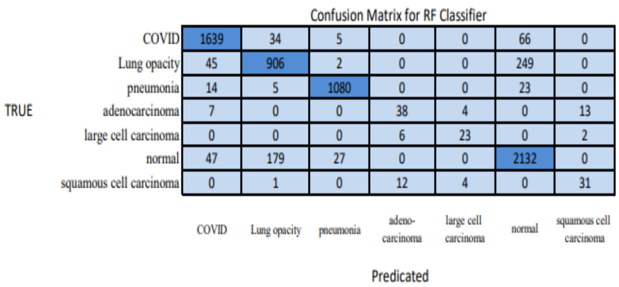

(d)

Figure 5. The confusion matrices for different Classifiers of the proposed Hybrid model

Received: October 23, 2024. Revised: December 1, 2024.

lung cancer cases into adenocarcinoma, squamous cell carcinoma, and large cell. The coding procedures were executed using Matlab R2021a on a Windows-based operating system (Windows 10 Pro) running on hardware with an Intel Core i7 processor, 64 GB of DDR5 RAM, and a 4 GB graphics card.

Following the training of the CNN, we acquired a feature vector comprising 256 values. This feature vector was subsequently used as input for the three used ML classifiers during both the training and testing phases. The proposed model's training parameters, including the initial learning rate and maximum epochs, have been set to 0.001 and 5, respectively. The coding for the proposed approach within the Matlab integrated development environment (IDE) was executed using training-test ratios of 80% - 20%.

The test accuracies of the CNN only and the proposed hybrid model combining CNN and ML techniques can be found in Table 4 for multiclass classification of lung diseases. The experimental model through using RF classifier for detecting depression achieved an accuracy of about 89%, surpassing the baseline CNN classifier's accuracy of 85.4%. While the CNN-Adaboost and CNN-voting

Table 5. Classifier results comparison

Classifier	Classes	Recall	Precision	F1 score	AUC
CNN	COVID-19	0.87	0.95	0.91	0.8645
	Lung Opacity	0.70	0.74	0.72	
	Pneumonia	0.94	0.98	0.96	
	Adenocarcinoma	0.63	0.60	0.61	
	Large cell carcinoma	0.77	0.53	0.63	
	Normal	0.90	0.81	0.85	
	Squamous cell carcinoma	0.50	0.68	0.58	
Adaboost	COVID-19	0.93	0.91	0.92	
	Lung Opacity	0.74	0.77	0.76	
	Pneumonia	0.96	0.96	0.96	
	Adenocarcinoma	0.60	0.74	0.66	0.8703
	Large cell carcinoma	0.55	0.63	0.59	
	Normal	0.87	0.86	0.87	
	Squamous cell carcinoma	0.71	0.59	0.60	
Voting	COVID-19	0.95	0.90	0.93	
	Lung Opacity	0.77	0.77	0.77	
	Pneumonia	0.96	0.96	0.96	
	Adenocarcinoma	0.66	0.62	0.64	0.8777
	Large cell carcinoma	0.71	0.73	0.72	
	Normal	0.86	0.89	0.87	
	Squamous cell carcinoma	0.54	0.68	0.60	
RF	COVID-19	0.94	0.94	0.94	0.8853
	Lung Opacity	0.75	0.81	0.78	
	Pneumonia	0.96	0.97	0.97	
	Adenocarcinoma	0.61	0.67	0.64	
	Large cell carcinoma	0.74	0.74	0.74	
	Normal	0.89	0.86	0.88	
	Squamous cell carcinoma	0.65	0.68	0.66	

Received: October 23, 2024. Revised: December 1, 2024.

achieved accuracies of about 87.3%, and 88% respectively which are still better than using the baseline CNN only model. This successful combination of CNN and ML classifier not only delivers strong results in lung diseases detection but also streamlines the feature extraction process, saving valuable time and effort. Figure shows the graphical representation of the accuracies of all used classifiers.

After completing the training process, the test confusion matrix results are presented in Fig. 5 for various classifiers, organized by class names. As shown in Fig. 5, the best COVID-19, lung opacity, and adenocarcinoma samples predictions have been achieved through using the voting ensemble ML classifier. Also, the best pneumonia and normal samples predictions have been achieved through using the RF ML classifier. For squamous cell carcinoma and large cell carcinoma, the classifiers that achieved best predictions are Adaboost and CNN, respectively. On the other hand, the worst COVID-19, lung opacity, pneumonia and squamous cell carcinoma samples predictions have been achieved through using CNN. The Adaboost ensemble ML classifier caused the worst predictions of adenocarcinoma, and large cell carcinoma. Finally, the worst normal samples predictions have been achieved through using voting ensemble classifier as shown in Fig. 5.

In assessing the efficiency of our proposed CNN method and ML models, we employed various metrics. Table 5 showcases these evaluation metrics for the proposed method. This paper also determined the results of using the baseline CNN model for classification of lung diseases to compare its results with respect to the ML classifiers.

In the results of CNN classifier, the best recall value was 0.94 for the Pneumonia class and the worst was 0.50 for the Squamous cell carcinoma class. The best precision was 0.98 for the pneumonia class and

Table 6. Results comparison with other methods

Model	Recall	Precision	F1 score	Accuracy
CNN-RF	0.96	0.97	0.97	**0.88**
RetinaNet and MaskR-CNN [14]	0.793	-	-	**-**
CNN [20]	-	-	0.82	**0.875**

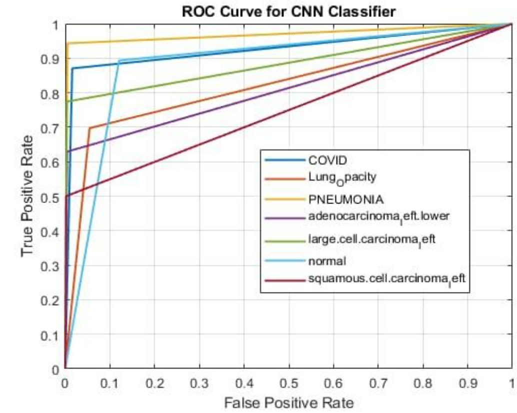

(a)

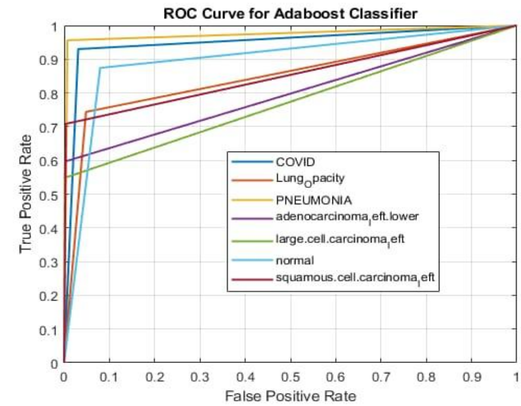

(b)

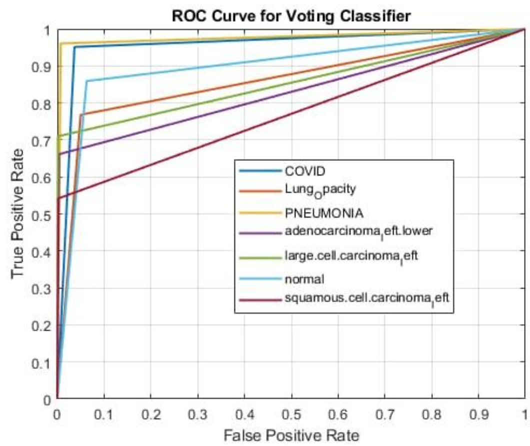

(c)

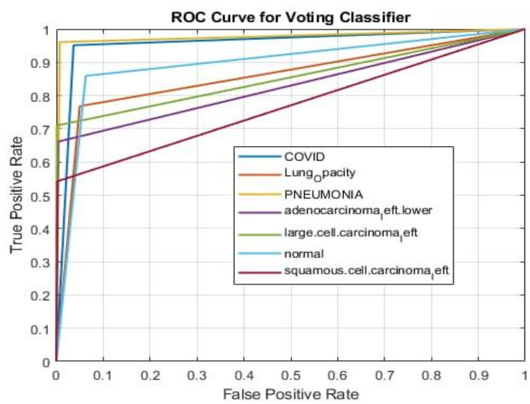

(d)

Figure. 6 The ROC Curves of all Classes in all Classifiers the worst was 0.53 for the large cell carcinoma class. The best F1-score was 0.96 for the Pneumonia class and the worst F-score was 0.58 for the squamous cell carcinoma class.

In the results of Adaboost ensemble ML classifier, the best and worst recall values were 0.96, and 0.55 for the pneumonia and large cell carcinoma classes, respectively. Also, the best and worst precision values were 0.96, and 0.59 for the pneumonia and squamous cell carcinoma classes, respectively. The best F1-score was 0.96 for the pneumonia class and the worst F-score was 0.59 for the large cell carcinoma class.

In the results of Voting ensemble ML classifier, the best and worst recall values were 0.96, and 0.54 for the pneumonia and squamous cell carcinoma classes, respectively. Also, the best and worst precision values were 0.96, and 0.62 for the pneumonia and Adenocarcinoma classes, respectively. The best F1-score was 0.96 for the pneumonia class and the worst F-score was 0.60 for the squamous cell carcinoma class.

In the results of RF ML classifier, the best and the worst recall, precision, and Fi score values were for the pneumonia and adenocarcinoma classes, as shown in Table 5. Where the best and the worst recall values were 0.96, and 0.61, respectively. Also, the best and the worst precision values were 0.97, and 0.67 respectively. Finally, the best F1-score was 0.97 for the pneumonia class and the worst F-score was 0.64 for the adenocarcinoma class.

The ROC graphs of all classes in each classifier have been represented in Fig. 6.

In conclusion, the results showcase the efficacy of the proposed multi-classification hybrid model in significantly improving accuracy and efficiency in detecting and classifying lung diseases. The integration of CNN and ML classifiers not only enhances disease prediction but also streamlines the feature extraction process, presenting a valuable contribution to the field of medical image analysis. The nuanced performance across different disease classes and the favorable evaluation metrics underscores the model's potential for real-world application in clinical settings, promising enhanced diagnostic capabilities and timely intervention.

5. Conclusion

This research demonstrates the application of DL with ML models to make informed predictions regarding lung diseases diagnosis. This paper introduces a multi-classification hybrid model for the detection of lung diseases such as pneumonia, COVID-19, lung opacity and lung carcinoma. As, CNN has been used as a feature extractor, while several ML classifiers have been applied for classification process. The suggested hybrid model is constructed through a series of steps, including pre-processing, robust feature extraction, and classification. For the actual detection of lung diseases from input chest X-ray images, various ML classifiers are employed.

The simulation results showed that the proposed CNN-RF model which used the RF as a classifier achieved the best accuracy of approximately 89%. This outperformed the baseline CNN classifier, which achieved an accuracy of 85.4%. Additionally, the CNN-Adaboost and CNN-voting approaches achieved accuracies of approximately 87.3% and 88%, respectively, still surpassing the performance of the baseline CNN-only model. This successful fusion of CNN and ML classifiers not only yields robust results in lung disease detection but also simplifies the feature extraction process, resulting in significant time and effort savings.

In the future, our plans include enhancing the model's accuracy by exploring alternative architectures and developing an implementation approach suitable for embedded systems.

We work on developing an implementation for real-world computer aided diagnosis using simple graphical user interface reaches a higher accuracy than the current one.

Conflicts of Interest

“The authors declare no conflict of interest.”

Author Contributions

Conceptualization, methodology, Mustafa Abdul Salam, Nabil Abdul Salam, Marwa Abdallah; software, Nabil Abul Salam, Mustafa Abdul Salam; validation, formal analysis, investigation, Mustafa Abdul Salam, Nabil Abdul Salam, Marwa Abdallah, Amr Abdellatif; resources, data curation, writing original draft preparation, review and editing, Mustafa Abdul Salam, Nabil, Marwa Abdallah; writing, visualization, Nabil Abdul Salam; supervision, project administration, Mustafa Abdul Salam, Nabil Abdul Salam, Marwa Abdallah, Amr Abdellatif; funding acquisition, Nabil Abdul Salam, Mustafa Abdul Salam.

Acknowledgments

The authors would like to thank the Deanship of Scientific Research, Prince Sattam Bin Abdulaziz University, Al-Kharj, Saudi Arabia, for supporting this research via funding from Prince Sattam Bin

Abdulaziz University project number (PSAU/2024/R/1445).

References

[1] W. J. Wiersinga, A. Rhodes, A. C. Cheng, S. J. Peacock, and H. C. Prescott, "Pathophysiology, Transmission, Diagnosis, and Treatment of Coronavirus Disease 2019 (COVID-19): A Review", *JAMA*, Vol. 324, No. 8, pp. 782-793, 2020, doi: 10.1001/JAMA.2020.12839.

[2] C. W. M. Ong *et al.*, "Epidemic and pandemic viral infections: impact on tuberculosis and the lung", *Eur. Respir. J.*, Vol. 56, No. 4, 2020, doi: 10.1183/13993003.01727-2020.

[3] K. Dhama *et al.*, "Coronavirus disease 2019-COVID-19", *Clin. Microbiol. Rev.*, Vol. 33, No. 4, pp. 1-48, 2020, doi: 10.1128/CMR.00028-20.

[4] "WHO/Europe | Coronavirus disease (COVID-19) outbreak", http://www.euro.who.int/en/health-topics/health-emergencies/coronavirus-covid-19 (accessed May 30, 2020).

[5] "Pneumonia and Diarrhoea Progress Report 2020 - NEXT IAS - Current Affairs Blog", https://blog.nextias.com/pneumonia-and-diarrhoea-progress-report-2020 (accessed Aug. 31, 2023).

[6] H. Sung *et al.*, "Global Cancer Statistics 2020: GLOBOCAN Estimates of Incidence and Mortality Worldwide for 36 Cancers in 185 Countries", *CA. Cancer J. Clin.*, Vol. 71, No. 3, pp. 209-249, 2021, doi: 10.3322/CAAC.21660.

[7] S. B. Knight, P. A. Crosbie, H. Balata, J. Chudziak, T. Hussell, and C. Dive, "Progress and prospects of early detection in lung cancer", *Open Biol.*, Vol. 7, No. 9, 2017, doi: 10.1098/RSOB.170070.

[8] "Rural Health Statistics 2020-21 | Ministry of Health and Family Welfare | GOI", https://main.mohfw.gov.in/newshighlights-90 (accessed Aug. 31, 2023).

[9] F. A. Mostafa, L. A. Elrefaei, M. M. Fouda, and A. Hossam, "A Survey on AI Techniques for Thoracic Diseases Diagnosis Using Medical Images", *Diagnostics*, Vol. 12, No. 12, 2022, doi: 10.3390/DIAGNOSTICS12123034.

[10] A. Hossam, A. Fawzy, B. E. Elnaghi, and A. Magdy, "An Intelligent Model for Rapid Diagnosis of Patients with COVID-19 Based on ANFIS", *Lect. Notes Data Eng. Commun. Technol.*, Vol. 100, pp. 338-355, 2022, doi: 10.1007/978-3-030-89701-7_30.

[11] A. M. Hasan, H. M. Abd El-Kader, and A. Hossam, "AN INTELLIGENT DETECTION SYSTEM FOR COVID-19 DIAGNOSIS USING CT-IMAGES", *JES. J. Eng. Sci.*, Vol. 49, No. No 4, pp. 476-508, 2021, doi: 10.21608/JESAUN.2021.61028.1031.

[12] S. H. Ahmed, A. Hossam, and B. M. ElHalawany, "Performance of Different Deep Learning Models for COVID-19 Detection", *Lect. Notes Data Eng. Commun. Technol.*, Vol. 113, pp. 78-88, 2022, doi: 10.1007/978-3-031-03918-8_8.

[13] S. Wankhade and V. S., "A novel hybrid deep learning method for early detection of lung cancer using neural networks", *Healthc. Anal.*, Vol. 3, p. 100195, 2023, doi: 10.1016/J.HEALTH.2023.100195.

[14] I. Sirazitdinov, M. Kholiavchenko, T. Mustafaev, Y. Yixuan, R. Kuleev, and B. Ibragimov, "Deep neural network ensemble for pneumonia localization from a large-scale chest x-ray database", *Comput. Electr. Eng.*, Vol. 78, pp. 388-399, 2019, doi: 10.1016/J.COMPELECENG.2019.08.004.

[15] K. El Asnaoui, Y. Chawki, and A. Idri, "Automated Methods for Detection and Classification Pneumonia Based on X-Ray Images Using Deep Learning", *Artificial Intelligence and Blockchain for Future Cybersecurity Applications. Studies in Big Data*, Vol 90, 2021, doi: 10.1007/978-3-030-74575-2_14.

[16] H. C. Reis and V. Turk, "COVID-DSNet: A novel deep convolutional neural network for detection of coronavirus (SARS-CoV-2) cases from CT and Chest X-Ray images", *Artif. Intell. Med.*, Vol. 134, 2022, doi: 10.1016/J.ARTMED.2022.102427.

[17] T. Rahman *et al.*, "Reliable tuberculosis detection using chest X-ray with deep learning, segmentation and visualization", *IEEE Access*, Vol. 8, pp. 191586-191601, 2020.

[18] C. H. Lin, C. J. Lin, Y. C. Li, and S. H. Wang, "Using generative adversarial networks and parameter optimization of convolutional neural networks for lung tumor classification", *Appl. Sci.*, Vol. 11, No. 2, pp. 1-17, 2021.

[19] S. M. Ashhar *et al.*, "Comparison of deep learning convolutional neural network (CNN) architectures for CT lung cancer classification", *Int. J. Adv. Technol. Eng. Explor.*, Vol. 8, No. 74, pp. 126-134, 2021.

[20] X. Ouyang *et al.*, "Dual-Sampling Attention Network for Diagnosis of COVID-19 From Community Acquired Pneumonia", *IEEE Trans. Med. Imaging*, Vol. 39, No. 8, pp. 2595-2605, 2020, doi: 10.1109/TMI.2020.2995508.

Received: October 23, 2024. Revised: December 1, 2024.

[21] M. M. Ahsan, T. E. Alam, T. Trafalis, and P. Huebner, "Deep MLP-CNN Model Using Mixed-Data to Distinguish between COVID-19 and Non-COVID-19 Patients", *Symm*, Vol. 12, No. 9, p. 1526, 2020, doi: 10.3390/SYM12091526.

[22] T. S. Qaid, H. Mazaar, M. Y. H. Al-Shamri, M. S. Alqahtani, A. A. Raweh, and W. Alakwaa, "Hybrid Deep-Learning and Machine-Learning Models for Predicting COVID-19", *Comput. Intell. Neurosci.*, Vol. 2021, 2021.

[23] Y. A. Nanehkaran, Zhu Licai, Junde Chen, Qiu Zhongpan, Yuan Xiaofeng, Yahya Dorostkar Navaei, Sajad Einy, "Diagnosis of Chronic Diseases Based on Patients' Health Records in IoT Healthcare Using the Recommender System", *Wireless Communications and Mobile Computing*, Vol. 2022, Article ID 5663001, 14 pages, 2022. doi.org/10.1155/2022/5663001

[24] X. Lu, Y. A. Nanehkaran, M. K. Fard, "A Method for Optimal Detection of Lung Cancer Based on Deep Learning Optimized by Marine Predators Algorithm", *Computational Intelligence and Neuroscience*, Vol. 2021, Article ID 3694723, 10 pages, 2021.

[25] G. V. E. Rao, P. N. Srinivasu, et al, "Hybrid framework for respiratory lung diseases detection based on classical CNN and quantum classifiers from chest X-rays", *Biomedical Signal Processing and Control*, Vol. 88, Part B, 2024, doi: 10.1016/j.bspc.2023.105567.

[26] P. Ramadevi and R. Das, "An Extensive Analysis of Machine Learning Techniques with Hyper-Parameter Tuning by Bayesian Optimized SVM Kernel for the Detection of Human Lung Disease", *IEEE Access*, Vol. 12, pp. 97752-97770, 2024.

[27] "Find Open Datasets and Machine Learning Projects | Kaggle", https://www.kaggle.com/datasets (accessed Sep. 05, 2023).

[28] T. Rahman *et al.*, "Exploring the effect of image enhancement techniques on COVID-19 detection using chest X-ray images", *Comput. Biol. Med.*, Vol. 132, 2021, doi: 10.1016/J.COMPBIOMED.2021.104319.

[29] "COVID-19 Radiography Database | Kaggle", https://www.kaggle.com/datasets/tawsifurrahman/covid19-radiography-database (accessed Sep. 05, 2023).

[30] L. Wang, J. Zhang, P. Liu, K. K. R. Choo, and F. Huang, "Spectral-spatial multi-feature-based deep learning for hyperspectral remote sensing image classification", *Soft Comput.*, Vol. 21, No. 1, pp. 213-221, 2017, doi: 10.1007/S00500-016-2246-3/FIGURES/6.

[31] K. Noda, Y. Yamaguchi, K. Nakadai, H. G. Okuno, and T. Ogata, "Audio-visual speech recognition using deep learning", *Appl. Intell.*, Vol. 42, No. 4, pp. 722-737, 2015, doi: 10.1007/S10489-014-0629-7/FIGURES/9.

[32] J. Hirschberg and C. D. Manning, "Advances in natural language processing", *Science*, Vol. 349, No. 6245, pp. 261-266, 2015, doi: 10.1126/SCIENCE.AAA8685.

[33] S. D. Bhinge *et al.*, "Formulation and evaluation of polyherbal gel containing extracts of Azadirachta indica, Adhatoda vasica, Piper betle, Ocimum tenuiflorum and Pongamia pinnata", *J. Res. Pharm.*, Vol. 23, No. 1, pp. 44-54, 2018.

[34] M. Schonlau and R. Y. Zou, "The random forest algorithm for statistical learning", *Stata J.*, Vol. 20, No. 1, pp. 3-29, 2020, doi: 10.1177/1536867X20909688/ASSET/IMAGES/10.1177_1536867X20909688-IMG8.PNG.

[35] H. S. Gurm, J. Kooiman, T. LaLonde, C. Grines, D. Share, and M. Seth, "A random forest based risk model for reliable and accurate prediction of receipt of transfusion in patients undergoing percutaneous coronary intervention", *PLoS One*, Vol. 9, No. 5, 2014, doi: 10.1371/JOURNAL.PONE.0096385.

[36] P. Panov and S. Džeroski, "Combining bagging and random subspaces to create better ensembles", *Lect. Notes Comput. Sci. (including Subser. Lect. Notes Artif. Intell. Lect. Notes Bioinformatics)*, Vol. 4723 LNCS, pp. 118-129, 2007, doi: 10.1007/978-3-540-74825-0_11.

[37] C. J. McWilliams *et al.*, "Towards a decision support tool for intensive care discharge: Machine learning algorithm development using electronic healthcare data from MIMIC-III and Bristol, UK", *BMJ Open*, Vol. 9, No. 3, 2019, doi: 10.1136/BMJOPEN-2018-025925.

[38] R. Patra, "Prediction of lung cancer using machine learning classifier", *Commun. Comput. Inf. Sci.*, Vol. 1235 CCIS, pp. 132-142, 2020.

[39] S. Kumari, D. Kumar, and M. Mittal, "An ensemble approach for classification and prediction of diabetes mellitus using soft voting classifier", *Int. J. Cogn. Comput. Eng.*, Vol. 2, pp. 40-46, 2021, doi: 10.1016/j.ijcce.2021.01.001.

[40] J. Qin, W. Pan, X. Xiang, Y. Tan, and G. Hou, "A biological image classification method based on improved CNN", *Ecol. Inform.*, Vol. 58, 2020.